

Research Paper

A lifecycle carbon emission evaluation model for urban underground highway tunnel facilities

Guosheng Wang^a, Dechun Lu^{a,*}, Gangao Ji^a, Xuhua Liang^a, Qingtao Lin^a,
Jirui Lv^b, Xiuli Du^a

^a Key Laboratory of Urban Security and Disaster Engineering of Ministry of Education, Beijing University of Technology, Beijing 100124, China

^b CCCC Tunnel Engineering Company Limited, Beijing 100102, China

Received 20 July 2024; received in revised form 9 April 2025; accepted 22 April 2025

Available online 18 July 2025

Abstract

Anthropogenic greenhouse gas emissions stand as the primary catalyst of climate perturbations. A precise evaluation of these emissions holds paramount importance in realizing energy conservation and emission reduction goals. Urban underground highway tunnel facilities emerge as a promising recourse for ameliorating traffic congestion and advancing energy conservation and emission mitigation endeavours. Nonetheless, the methodologies for quantifying its carbon emissions remain scant. This study ventures into the realm of carbon footprint appraisal within the lifecycle paradigm of underground highway tunnel facilities. Tailored to the characteristics, functionalities, and design intricacies of urban underground highway tunnel facilities, the physical boundaries and scopes are meticulously calibrated. Subsequently, a carbon emission computational model adept at encapsulating the emission characteristics throughout the entire lifecycle is formulated. Meanwhile, a detailed database is established for emission factors of various carbon emission activities. Leveraging insights garnered from a specific project case, the overarching carbon emission profiles of the urban underground highway tunnel facility, both in aggregate and individual stages, are elucidated. Concomitantly, bespoke recommendations and strategies aimed at energy preservation and emission abatement are proffered, attuned to the idiosyncratic attributes of carbon emissions across distinct stages.

Keywords: Urban underground highway tunnel; Carbon emission; Entire lifecycle; Calculation model; Energy saving and emission reduction

1 Introduction

Climate change stands as a formidable and urgent global challenge, rallying considerable attention and concerted efforts from the international community. Principal contributors to this predicament encompass fossil fuel utilization, land use alterations, and the emission of greenhouse gases stemming from industrial pursuits (Prather et al., 2009). In China, the transportation sector's carbon emissions accounted for approximately 11% of the total carbon

output in 2019 (Center for Strategic Studies of the Chinese Academy of Engineering et al., 2022), emerging as one of the pivotal sources of urban carbon footprint (Li et al., 2021). With the continuous growth in demand for transportation infrastructure, an increasing number of projects venture underground to expand infrastructure capacity, optimize land utilization, and enhance green spaces in urban environments. Urban underground highway tunnels can increase the capacity of the urban road network by more than 30%, and the operating mileage of these tunnels continues to grow steadily each year. Consequently, the imperative arises to establish a robust methodology for comprehensively assessing the lifecycle carbon emissions of urban underground highway tunnel facilities, enabling

* Corresponding author.

E-mail address: dechun@bjut.edu.cn (D. Lu).

Peer review under the responsibility of Tongji University

Nomenclature

AM	actual measurement	ECU	equipment carbon use (consumption)
CP	construction process	LCA	life cycle assessment
CS	carbon source	MP	building material production
CU	carbon use (consumption)	MT	building material transportation
CF	carbon fixation	OM	operation and maintenance
CM	construction materialization	VCU	vehicle carbon use (consumption)
CEF	carbon emission factor		

accurate evaluation of the transportation sector's carbon equivalence and facilitating the formulation of pertinent energy-saving and emission-reduction strategies.

Carbon emission assessment utilizes various methods, including inventory analysis, actual measurement (AM), input–output, progress analysis, and life cycle assessment (LCA). The inventory analysis method calculates the carbon equivalence of each inventory component, mainly used for micro-scale carbon emission calculations (Lee et al., 2020). The AM requires specific methods to measure on-site emission concentrations and flow rates and calculate carbon emissions according to relevant standards, but its application is not widespread (Liu et al., 2019; Nyhan et al., 2016). The input–output method primarily determines the consumption coefficients of specific departments for economic analysis. Although it is suitable for macro-level carbon emission calculations, its accuracy is generally moderate (Qi et al., 2022). The progress analysis method has the advantage of simple calculation and can decompose carbon emissions from specific processes. However, the secondary connection is often ignored in the segmentation process, resulting in truncation errors in the calculation results (Aye et al., 2012). The LCA method analyzes the entire lifecycle and provides effective emission reduction recommendations. LCA is widely applied in carbon footprint assessments across different domains and products (Guo et al., 2024; Peng et al., 2024; Su et al., 2023).

Since its application in construction in 1990, LCA has become a key method for evaluating building environmental impacts. Early works, such as Zhang (2002), introduced simplified LCA methods to overcome the complexities of data collection and lifecycle evaluation, segmenting the process into six stages: material production, transportation, construction, use, maintenance, demolition, and recycling. Other studies, such as Gustavsson et al. (2010) and Cole (1998), proposed alternative stages, while Chen et al. (2011) expanded the lifecycle into nine stages, highlighting its modularity. In assessing the carbon footprint of above-ground buildings, the operational stage is typically the largest contributor, accounting for 60%–80% of total lifecycle emissions (Pan et al., 2023). Accordingly, many studies focus primarily on this stage (Ghafoori & Abdallah, 2022; Mohamed, 2019). LCA has also been applied to transportation systems, with Ghate and Qamar (2020) comparing the energy efficiency of India's urban transit systems, demon-

strating subways' greater potential for emission reduction. Similarly, Pérez et al. (2017) analyzed Madrid's waste collection fleet, identifying fuel consumption as the main source of emissions. These findings facilitated the development of strategies for emission reduction. However, applying these aboveground frameworks directly to urban underground highway tunnel risks omitting key factors such as carbon fixation and emissions from underground engineering activities. Several studies have made significant progress in developing LCA-based methods for assessing carbon emissions in urban underground spaces. For example, Li et al. (2018) evaluated the carbon emissions of a Shanghai subway section, providing a relatively comprehensive lifecycle assessment, though only two main materials were considered. Wu et al. (2024) applied LCA to a cross-sea tunnel in the Guangdong-Hong Kong-Macao region, offering a reasonable system boundary delineation but without accounting for carbon fixation. Qiao et al. (2019) proposed a low-carbon framework for urban underground spaces, though material production and construction stages were not addressed. Wang et al. (2025) examined carbon emissions during the construction stage of underground facilities and considered carbon fixation from increased green space, though emissions during the construction materialization stage were not included. While these studies have laid a solid foundation for understanding the lifecycle carbon emissions of specific underground facilities, challenges remain in terms of system boundary completeness, availability of emission factor data, and coverage of all lifecycle stages. Developing more comprehensive methods would enable a more accurate assessment of carbon emissions across the entire lifecycle of urban underground highway tunnel facilities.

In response to these gaps, this study seeks to define appropriate carbon footprint boundaries and scales for urban underground highway tunnel facilities. A corresponding calculation model is proposed, along with a tailored carbon emission calculation method. Practical insights from engineering applications are utilized to identify emission patterns, providing guidance for energy-saving and emission-reduction strategies.

2 Carbon emission calculation model for urban underground highway tunnel facility

At the heart of the lifecycle calculation model lies the delineation of the physical boundary and spatial–temporal

scale for the carbon footprint of the research subject. Capitalizing on the distinctive attributes of urban underground highway tunnel facilities, the physical boundary is demarcated into three tiers.

2.1 Physical boundaries

The lifecycle stages of urban underground highway tunnel facilities can be categorized into the design stage, construction materialization (CM) stage, operation and maintenance (OM) stage, and disposal stage, similar to aboveground buildings (Fenner et al., 2018; Sim & Sim, 2017; Teng & Wu, 2014). However, carbon emissions during the initial design stage have minimal impact on the overall lifecycle emissions in urban underground highway tunnel facilities, approximately 5% of the entire lifecycle (Li & Chen, 2020). The carbon emissions during the design stage mainly involve drawing design, material selection, etc., which are mostly generated by personnel work activities and are difficult to track. Therefore, following the Pareto rule, carbon emissions from the design stage can be disregarded from the carbon footprint analysis (Richard, 2001). Additionally, underground space development is irreversible (Peng et al., 2021), making it challenging to demolish and rebuild underground infrastructure like aboveground buildings. Hence, carbon emissions during this stage are considered part of the construction stage for new or renovated infrastructure (Qiao et al., 2024). Consequently, the lifecycle calculation boundary for urban underground highway tunnel facilities is divided into the construction materialization stage and operation and maintenance, forming the primary boundary (Fig. 1).

In the construction materialization stage, the carbon footprint can be divided into building materials activities and infrastructure construction activities based on types of engineering activities. Building materials activities include the production and transportation processes of building materials, as shown in Fig. 1(a). Across the entire life cycle of urban underground road tunnel infrastructure, the operation and maintenance stage contributes the largest share of total carbon emissions. These emissions primarily stem from the carbon consumption end and the carbon sequestration end. The carbon source end, in this context, refers to the indirect emissions generated to meet the energy demands of the carbon consumption end, encompassing both fossil-based and clean energy sources. Given that the energy consumption of underground highway tunnel facilities directly determines the corresponding energy supply, and in accordance with the law of energy conservation, energy loss during conversion processes is inevitable. To quantify the extent of such losses, this study introduces an energy loss coefficient. When no loss occurs during energy conversion, the coefficient is assigned a value of 1; if losses are present, the coefficient should be determined based on the actual energy conversion efficiency. However, detailed estimation of these losses would considerably increase the complexity of data collection and computational analysis. Therefore, for the sake of simplification, this study assumes the energy loss coefficient to be 1, ignoring the impact of energy loss on carbon emissions. Furthermore, to avoid double counting, the carbon emissions during the operation and maintenance stage are accounted for solely based on direct emissions from the carbon consumption end. The carbon fixation end refers to carbon dioxide absorbed by released ground space as

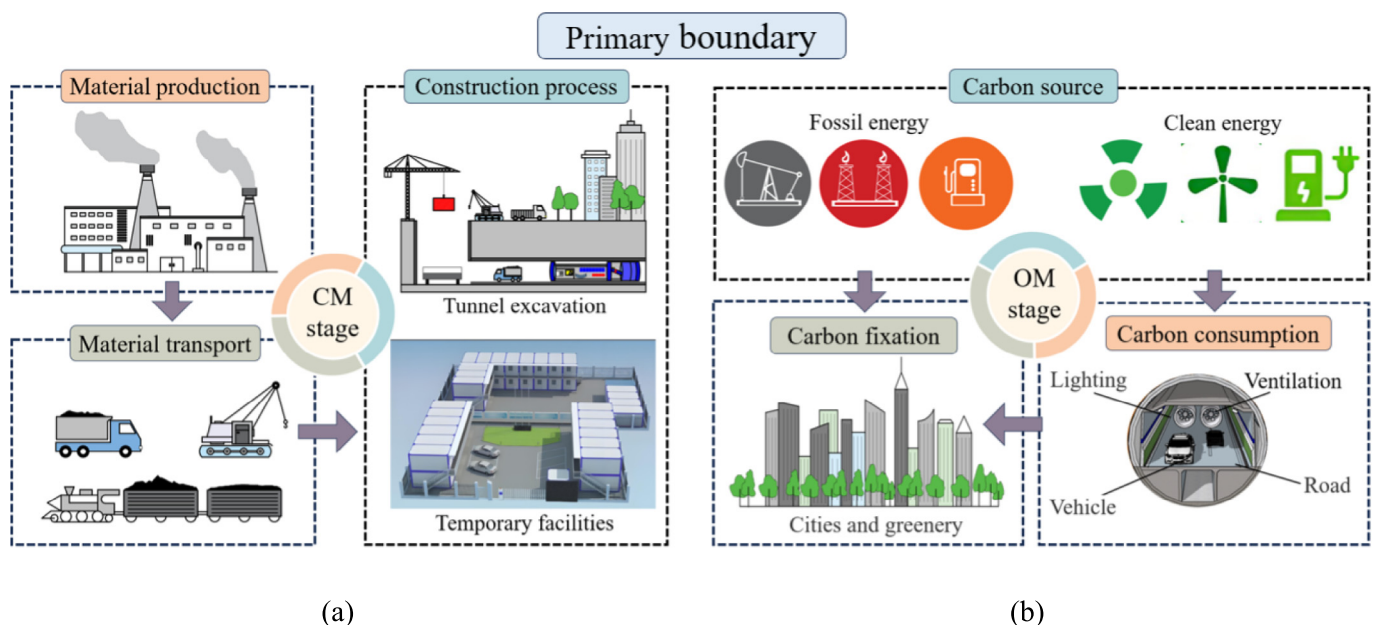


Fig. 1. Primary boundary of lifecycle carbon emission for the tunnel facility. (a) Carbon footprint distribution during the construction materialization stage, and (b) three end carbon emission system during operation and maintenance stage.

urban green space or through carbon sequestration technology. More details on the carbon source end, carbon consumption end, and carbon fixation end in the operation and maintenance stage are presented in Fig. 1(b). Thus, the building materials activity, construction activity, carbon source end, carbon consumption end, and carbon fixation end are defined as the secondary boundary.

According to the activity list in the urban underground highway tunnel facilities, the secondary boundary expands to form a tertiary boundary for the carbon footprint, as shown in Fig. 2. The primary boundary includes the CM stage and the OM stage. The secondary boundary refines the primary boundary, incorporating carbon emissions from building materials activities, construction activities, source-end carbon emissions, consumption-end carbon emissions, and carbon fixation-end carbon absorption. The tertiary boundary provides further details on specific production and activities. Building materials activities involve materials like steel, concrete, cement, and transportation modes such as roads, railways, waterways, and airfreight. Infrastructure construction activities cover both above ground and underground construction, including preparation work, operation of construction equipment, and temporary facilities. It is worth noting that temporary facilities will generate carbon emissions during the construction stage, and can offset part of the carbon emissions from material production during the recycling stage. Since the boundary of the calculation model in this paper does not consider the consumption stage, and the carbon emissions from this part of material recovery are relatively small compared with the production stage, we will consider

this part of offset emissions into the emission factor of material production stage. Underground construction includes excavation engineering, earthworks engineering, structural engineering, and drainage works. In the operation and maintenance stage, the carbon source end mainly includes emissions from fossil fuels and clean energy sources like solar energy, wind energy, and geothermal energy. The carbon consumption end consists of carbon emissions from vehicles (gasoline, diesel, electric, and hybrid) and infrastructure auxiliary equipment (lighting systems, ventilation systems, and facilities maintenance). The carbon fixation end involves capturing and storing carbon dioxide through physical carbon sequestration (underground or deep-sea deposition) and biological carbon fixation (binding carbon dioxide in plants or microorganisms).

2.2 Temporal and spatial scale

The spatial scale of urban underground highway tunnel facilities is measured primarily by the tunnel’s length and width, while the temporal scale encompasses both the construction and operation stages of the transportation system. Therefore, defining the computational scale of urban underground highway tunnel facilities requires a dual consideration of spatial and temporal dimensions, which is essential for accurately assessing the energy and resource consumption associated with such facilities. In China, the construction stage typically lasts 2–5 years, and the operation and maintenance stage can extend up to 100 years (Barles, 2009; Li et al., 2008). The influence of spatial

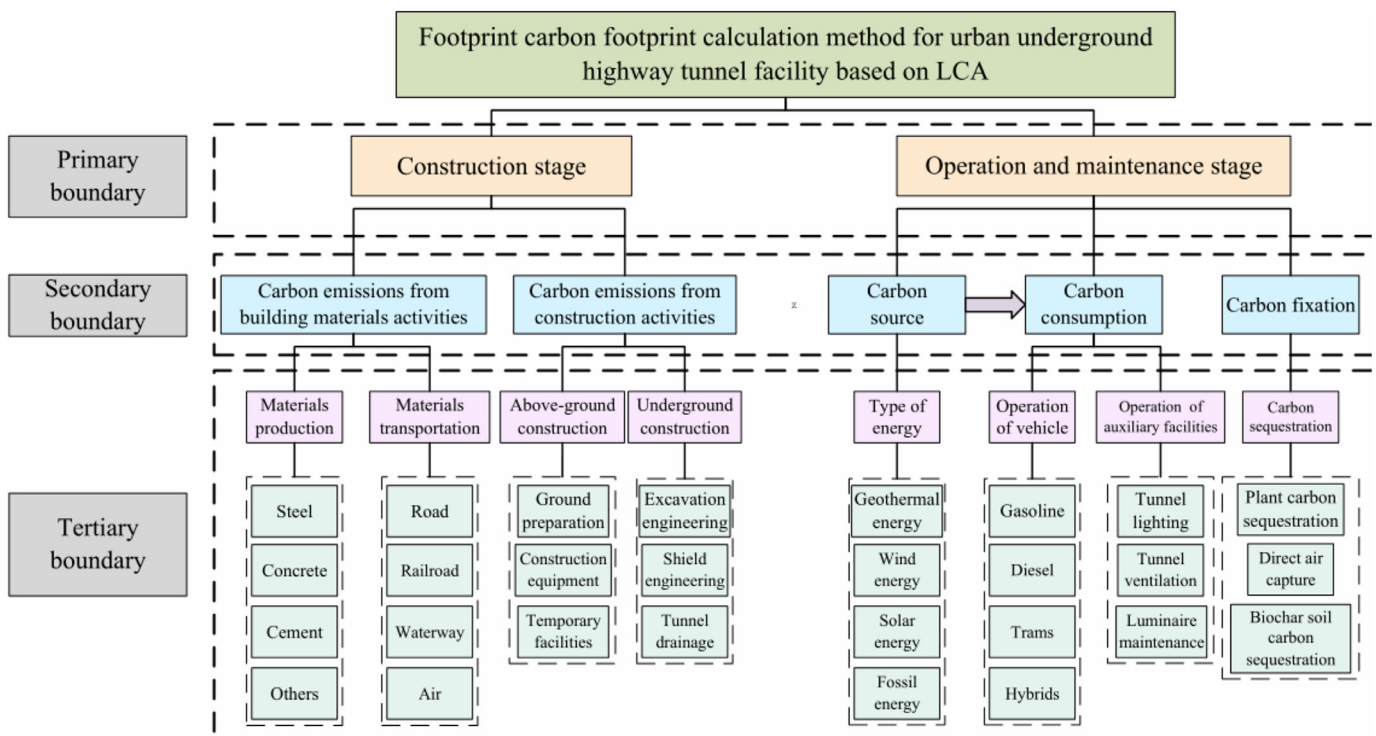


Fig. 2. Schematic diagram of the lifecycle of underground highway tunnel facilities.

and temporal scales can be illustrated using lighting systems as an example. To accurately calculate the carbon emissions from lighting infrastructure, it is necessary to determine the quantity and operating duration of the devices. By multiplying the energy consumption factors per unit of time and distance by the tunnel length (spatial scale) and operational time (temporal scale), the carbon emissions from the lighting equipment can be accurately calculated.

3 Carbon emission calculation method

Applying the LCA method of carbon footprint outlined in ISO 14042 (Finkbeiner et al., 2006), and incorporating the calculation boundaries and scales specified for urban underground highway tunnel facilities in Section 2, the carbon emission equivalent for the entire lifecycle of urban underground highway tunnel facilities can be articulated within the primary boundary as follows:

$$C_{LC} = C_{CM} + C_{OM}, \quad (1)$$

where C_{LC} denotes the overall carbon emissions across the complete lifespan of the underground highway tunnel facilities. Meanwhile, C_{CM} and C_{OM} signify the carbon emissions during the construction materialization stage and operation and maintenance, respectively, measured in kilograms of carbon dioxide equivalent (kgCO₂e).

3.1 Construction materialization stage

Based on the calculation boundary defined in Section 2.1, the construction materialization stage comprises three specific activities: building material production (MP), building material transportation (MT), and the construction process (CP). Therefore, we can express C_{CM} as

$$C_{CM} = C_{MP} + C_{MT} + C_{CP}, \quad (2)$$

where C_{MP} , C_{MT} , and C_{CP} individually signify the carbon emissions resulting from the production, material transportation, and construction processes of building materials during the construction materialization stage, whose formulations can be expressed as

$$C_i = \sum_{j=1}^m Q_{ij} \cdot f_{ij}, \quad (3)$$

where C_i denotes the carbon emissions produced in the i sub-stage of the construction materialization stage, with i taking the values of material production, building material transportation, and the construction process. Q_{ij} denotes the consumption of the j energy or material in the i stage of the secondary boundary, with the standard weight unit being typically t, the length unit usually m, and the volume unit typically m³. f_{ij} represents the carbon emission factor (CEF) of the j energy or material in the i stage, expressed as kgCO₂e per activity unit. The variable m stands for

the total number of engineering activities generating carbon emissions in a particular stage. Equation (3) assumes constant energy utilization efficiency throughout the entire lifecycle.

When i equals MP, C_{MP} represents the carbon emissions arising from the production process of building materials. In Eq. (3), $Q_{MP,j}$ denotes the weight of building materials consumed by the infrastructure. To distinguish from other activities, M_j is used instead of $Q_{MP,j}$, where j signifies the type of building materials. $f_{MP,j}$ indicates the greenhouse gas emissions per unit mass or volume of building materials during production or extraction, encompassing carbon emissions resulting from energy combustion and carbon emissions originating from physical or chemical reactions within the process. Consequently, Eq. (3) can be rephrased as follows:

$$C_{MP} = \sum_j M_j \cdot f_{MP,j}, \quad (4)$$

where $f_{MP,j}$ is the carbon emission factor associated with the production of building materials. This paper utilizes the carbon emission factor for building materials production outlined in the Standard for building carbon emission calculation (Ministry of Housing and Urban-Rural Development of the People's Republic of China, 2019), detailed in Table A1.

When i is equal to MT, C_{MT} indicates the carbon emissions incurred during the transportation of building materials. In Eq. (3), $Q_{MT,j}$ is influenced by both the weight of the building materials and the distance of transportation. To account for the combined effects of these factors, $Q_{MT,j}$ is expressed as follows:

$$Q_{MT,j} = M_j \cdot D_j, \quad (5)$$

where M_j signifies the weight of the building material, as mentioned in Eq. (4), while D_j represents the transportation distance of the building material. $f_{MT,j}$ in Eq. (3) denotes the carbon emissions produced per unit mass of building materials per unit of transportation distance. Thus, incorporating Eq. (5) into Eq. (3) results in

$$C_{MT} = \sum_j M_j \cdot D_j \cdot f_{MT,j}, \quad (6)$$

where $f_{MT,j}$ is the carbon emission factor associated with the transportation of building materials. Derived from the Standard for building carbon emission calculation (Ministry of Housing and Urban-Rural Development of the People's Republic of China, 2019), the carbon emission factors for different transportation modes are outlined in Table A2.

When i takes the value of CP, C_{CP} denotes the carbon emissions incurred during the construction process. In Eq. (3), $Q_{CP,j}$ represents the operational hours of the construction equipment. To distinguish from other activities, G_j is used instead of $Q_{CP,j}$, where j indicates the type of construction equipment. $f_{CP,j}$ signifies the greenhouse gas emissions produced by the construction equipment per unit

of time. Consequently, Eq. (3) can be reformulated as follows:

$$C_{CP} = \sum_j G_j \cdot f_{CP,j}, \quad (7)$$

where $f_{CP,j}$ is the carbon emission factor related to the operation of construction machinery. Consultation of the Standard for building carbon emission calculation (Ministry of Housing and Urban-Rural Development of the People's Republic of China, 2019) and Pi (2016) gives the carbon emission factor for construction machinery, as outlined in Table A3.

3.2 Operation and maintenance stage

Based on the operation and maintenance stage boundary specified in Section 2.1, carbon-related activities during this stage include both emission and fixation quantities. Emission quantities can be calculated from either the carbon source (CS) or the carbon use (CU), while fixation quantities can be determined by the carbon fixation (CF). Therefore, we define C_{OM} as

$$C_{OM} = C_{CU} + C_{CF}, \quad (8)$$

where C_{CU} is the carbon emission generated by the consumption and use (CU) at the operation and maintenance stage, and C_{CF} is the fixed carbon emission at the carbon fixation end, in kgCO_2e . Without accounting for variations in energy utilization efficiency, the carbon emissions from the carbon consumption end and the carbon source end are equivalent, and either can be utilized to represent the carbon emissions generated during the operation and maintenance stage, hence $C_{CU} = C_{CS}$. The formulations for C_{CS} , C_{CU} , and C_{CF} remain consistent with Eq. (3), except that the variables i are now $i = \text{CS}$, CU , and CF .

When i takes the value of carbon source, C_{CS} indicates the carbon emissions generated at the carbon source end. In Eq. (3), $Q_{CS,j}$ denotes the energy supply and consumption at the carbon source end of the infrastructure, which is replaced by E_j in order to distinguish it from other activities, j represents the type of energy. $f_{CS,j}$ signifies the greenhouse gas emissions released per unit mass of energy. Consequently, Eq. (3) can be converted into the following form:

$$C_{CS} = \sum_j E_j \cdot f_{CS,j}, \quad (9)$$

where $f_{CS,j}$ is the carbon emission factor associated with the type of energy supply. Referencing the Standard for building carbon emission calculation (Ministry of Housing and Urban-Rural Development of the People's Republic of China, 2019) and available literature (Gao et al., 2021), the carbon emission factors for various energy types are detailed in Table A4.

When i is set as CU, C_{CU} signifies the carbon emissions produced at the carbon consumption end. Figure 2 shows that the carbon emissions at the carbon consumption end

of urban underground highway tunnel facilities encompass both vehicle carbon consumption (VCU) and infrastructure auxiliary equipment carbon use (ECU). The carbon emission calculation model used in this study is based on frameworks developed for ground transportation infrastructure, where vehicle emissions are typically included in the overall carbon footprint of the system (Fenner et al., 2018; Liu et al., 2019; Ghate et al., 2020). On the other hand, the construction of underground highway tunnel facilities often alters the existing traffic network and carbon emission patterns. These changes, whether through reduced congestion or modified traffic routes, can impact the city's overall emissions. By including vehicle emissions, it is possible to more comprehensively assess the environmental impact throughout the infrastructure's lifecycle. Therefore, the C_{CU} can be further broken down into

$$C_{CU} = C_{VCU} + C_{ECU}, \quad (10)$$

where C_{VCU} and C_{ECU} represent the carbon emissions from vehicle operation and auxiliary equipment operation, respectively. By incorporating the activities of the tertiary boundary during vehicle operation, as illustrated in Fig. 2, into Eq. (10), we can derive

$$C_{VCU} = \sum_{j=1}^m Q_{VCU,j} \cdot f_{VCU,j}, \quad (11)$$

where $f_{VCU,j}$ signifies the greenhouse gas emissions produced per unit distance of the vehicle, where j denotes the energy type of the vehicle. Meanwhile, $Q_{VCU,j}$ represents the energy consumption during vehicle operation, which is affected by factors such as daily traffic flow (F_d), vehicle operating time (T), congestion coefficient (c), vehicle type proportion (P_j), and tunnel length (L_j). Accounting for these factors, $Q_{VCU,j}$ can be expressed as follows:

$$Q_{VCU,j} = c \cdot F_d \cdot T \cdot \sum_j P_j \cdot L_j. \quad (12)$$

By substituting Eq. (12) into Eq. (11), we obtain:

$$C_{VCU} = c \cdot F_d \cdot T \cdot \sum_j P_j \cdot L_j \cdot f_{VCU,j}, \quad (13)$$

where $f_{VCU,j}$ is the carbon emission factor for vehicles of various energy types. Consultation of the 2020 China Automotive Low Carbon Action Plan research report (China Automotive Data Co., Ltd., 2020) gives the unit distance carbon emission factor for vehicles of different energy types, as outlined in Table A5.

By incorporating the activities associated with the tertiary boundary during the operation of infrastructure auxiliary equipment, as depicted in Fig. 2, into Eq. (10), we can derive:

$$C_{ECU} = \sum_{j=1}^m Q_{ECU,j} \cdot f_{ECU,j}, \quad (14)$$

where $f_{ECU,j}$ denotes the carbon emissions from infrastructure auxiliary equipment per unit of time and distance, and

$Q_{ECU,j}$ represents the operational hours of all auxiliary equipment within the length range of the infrastructure.

Following the calculation scale outlined in Section 2.2, $Q_{ECU,j}$ can be expressed as the product of the operating time of all auxiliary equipment per unit distance and the length of the infrastructure:

$$Q_{ECU,j} = R_j \cdot L_j, \quad (15)$$

where R_j represents the total operating duration of all auxiliary equipment per unit distance, and L_j represents the length of the tunnel. Similar to Eq. (13), by substituting Eq. (15) into Eqs. (14) and (16) can obtain:

$$C_{ECU} = \sum_j R_j \cdot L_j \cdot f_{ECU,j}, \quad (16)$$

where $f_{ECU,j}$ represents the carbon emission factor of auxiliary infrastructure equipment. Regarding the arrangement of tunnel lighting facilities, single-sided lighting is generally adopted for two-lane tunnels, while symmetrical double-sided lighting is required for tunnels with four or more lanes to ensure sufficient illumination. According to the Guidelines for Design of Lighting of Highway Tunnels (China Merchants Chongqing Transportation Research and Design Institute., 2014), the placement of lighting fixtures must ensure a minimum visual flicker frequency of 16 Hz to avoid driver discomfort and ensure safety. As a result, the spacing of individual lighting fixtures, S , can be expressed as

$$S = \frac{v_t}{f}, \quad (17)$$

where f represents the flicker frequency and v_t corresponds to the design speed. In this study, a flicker frequency of $f = 20$ Hz is selected. Additionally, the power of a single lighting device selected in this article is 150 W. Regarding ventilation systems, the Guidelines for Design of Ventilation of Highway Tunnels (China Merchants Chongqing Transportation Science and Technology Design Institute Co., Ltd., 2014) stipulate that jet fans should be installed at standard intervals of 150 m. Typically, one to three sets of ventilation equipment are arranged at each cross-section. For long tunnels exceeding 3 km in length, the rated power of a single set of ventilation equipment generally exceeds 55 kW. Based on the installation density, the total energy consumption per kilometre of the tunnel ventilation system can be calculated. The detailed values are presented in Table A7. By multiplying the energy consumption per unit time and per unit length with the electricity emission factor, the carbon emission factors of tunnel lighting and ventilation systems can be further derived. The value of the electricity emission factor is significantly influenced by the regional power generation mix; regions dominated by fossil fuel-based electricity tend to have higher emission factors. Therefore, carbon emission assessments should adopt region-specific emission factors that reflect the local power grid structure. According to the most recent data released by China's Ministry of Ecology and

Environment, the current national average electricity emission factor is 0.585 kgCO₂e/kWh. Based on this value, the carbon emission factors for lighting and ventilation systems in Chinese tunnels are calculated accordingly, as shown in Tables A6 and A7. Zou (2013) projected the service life of lighting equipment to be 23 645 h using the spectral power distribution (SPD) method. This leads to a carbon emission coefficient for equipment maintenance of 0.53 kgCO₂e per kilometre per hour.

When i is set as CF, C_{CF} represents the quantity of carbon fixation absorbed by the carbon fixation end. In Eq. (3), $f_{CF,j}$ denotes the amount of green space carbon fixation absorbed per unit area and unit time. $Q_{CF,j}$ is influenced by the green space carbon fixation area and service life. To account for both factors, $Q_{CF,j}$ is articulated as follows:

$$Q_{CF,j} = A_j \cdot T, \quad (18)$$

where A_j denotes the green space area created through the underground renovation of the infrastructure, while T represents the operational time of the infrastructure.

By incorporating Eq. (18) into Eq. (3), we derive:

$$C_{CF} = \sum_j A_j \cdot T \cdot f_{CF,j}, \quad (19)$$

where $f_{CF,j}$ is the carbon absorption coefficients associated with the green space carbon fixation. Xu et al. (2023) supplied the annual carbon fixation per unit area for various types of vegetation in Beijing, detailed in Table A8.

According to the research conducted by Xu et al. (2023), the carbon fixation per unit area per year of various types of vegetation in Beijing is listed in Table A8.

4 Engineering case analysis

Taking an underground highway tunnel facility in Beijing as a case, the carbon footprint calculation method for the developed urban underground highway tunnel facility is applied to obtain the carbon emission equivalent of the project across various stages. The distribution and regional location of the project are shown in Fig. 3.

4.1 Project overview

A roadway in Beijing, initially built in December 1998 and opened to traffic in September 2001, adhered to highway standards. Plans have been made to upgrade the road to a two-way six-lane road in 2021, including the construction of an underground tunnel. The project involves two main sections: widening the road and improving the underground area. The underground renovation section spans 9.16 km, featuring a two-hole tunnel with upper and lower branches. The net width of a single-hole tunnel is 13 m, accommodating a two-way six-lane road with a speed limit of 80 km/h. Additionally, three sets of ventilation equipment are installed at each tunnel cross-section. The reclaimed ground space will be transformed into a 50-

Table 1
Consumption of building materials and corresponding transportation distance.

Number	Type of building materials	Material quantity	Transportation distance (km)	Number	Type of building materials	Material quantity	Transportation distance (km)
1	Bentonite	7123.3 t	1079.4	11	Concrete	456 172.4 m ³	40
2	Stabilizer	86.4 t	1158.5	12	Steel	163 563.1 t	500
3	Shield tail oil	1154.8 t	349.5	13	Gear oil	91.6 t	324.2
4	Grease	52.2 t	247.8	14	Waterproof material	6054.9 m ²	500
5	Staircase tiles	35.1 m ³	500	15	Fireproof material	190 788.4 m ²	500
6	Hydraulic oil	57.7 t	400.1	16	Clay stock	277.1 t	1836.4
7	Diesel oil	401.7 t	1060.8	17	Pipe	21.1 t	500
8	Tunneling agent	261.0 t	155.3	18	Building blocks	2813.7 m ³	500
9	Aluminum	626.3 t	500	19	Cement mortar	77.7 m ³	500
10	Cement	33 900.8 t	107.7	20	Water glass	13 927.6 t	107.7

Table 2
Construction machinery workload.

Number	Construction machinery	Workload	Unit	Number	Construction machinery	Workload	Unit
1	Excavator	60 630	m ³	5	Forklift	173 842.2	kg
2	Shield	7343.9	m	6	Mixer	401 792	kWh
3	Double-end truck	8 760 000	kWh	7	Boom lift truck	425 152	kWh
4	Tanker	184 368.8	kg	8	Electricity consumption	24 560 349.9	kWh

Table 3
Energy consumption factors for vehicle OM.

Number	Vehicle energy type	Vehicle proportion (%)	Number	Vehicle energy type	Vehicle proportion (%)
1	Electric	2.51	4	Natural gas	1.90
2	Hybrid	0.64	5	Gasoline	69.93
3	Gasoline	5.64	6	Motorcycle	19.38

artificial light is essential for 24-h driving safety (Zhao et al., 2022). Additionally, tunnel ventilation requires full line ventilation every 2 h, running for 1.5 h per operation, totaling 10.29 h per day (Liu, 2023). Carbon emissions from auxiliary equipment can be calculated using the 100-year infrastructure service life and 9.16 km infrastructure length in the relevant equation. Determining carbon fixation data requires identifying the green space area and infrastructure operation time resulting from the underground highway tunnel facility renovation. According to Beijing's project plan, about 50 ha of the released land will be transformed into urban parks and green spaces, with a service life of 100 years for the infrastructure. Carbon absorption from urban green spaces post-renovation can be calculated using the above values. Technologies like direct air capture and biochar soil carbon sequestration can enhance carbon fixation ability. The ventilation system can incorporate direct air capture technology for carbon sequestration in this project (Wang & Wang, 2022).

4.3 Carbon emission calculation results

The carbon emissions for different stages are obtained by substituting data from each table in Section 4.2 into

the corresponding calculation formula in Section 3. Results for construction materialization stage, operation and maintenance stage, and sub-stages are detailed in Table 4 and shown in Fig. 4. Analysis of the figure reveals that the largest portion of carbon emissions in the construction materialization stage comes from building materials production, accounting for 1 170 290.05 tCO₂e or 21.47% of the overall lifecycle emissions. In the subsequent construction stage, concrete and reinforcing steel are the primary building materials, with concrete relying on a cement-based matrix as its core binding component. During cement production, limestone undergoes thermal decomposition at high temperatures, releasing a substantial amount of carbon dioxide, making it a significant source of carbon emissions. Statistics indicate that approximately 0.51 tons of CO₂ are emitted for every ton of cement clinker produced; Steel, which usually uses iron ore as a raw material, also produces large amounts of carbon dioxide in the reduction reaction. In most materials production processes, high temperature heating is the most common method, and this process also consumes a lot of fossil energy and produces a lot of carbon dioxide. Construction activities contribute approximately 1.16% of emissions. In the operation and

Table 4
Carbon emissions calculation results for the entire lifecycle of the engineering case.

Primary boundary	Carbon emissions (tCO ₂ e)	Secondary boundary	Carbon emissions (tCO ₂ e)	Tertiary boundary	Carbon emissions (tCO ₂ e)
Materialization stage	1 247 540.98	Materials activities	1 184 147.55	Material production (MP)	1 170 290.05
		CP activities	63 393.43	Material transportation (MT)	13 857.51
Operation and maintenance stage	4 087 045.47	CU end	4 117 725.47	Construction process (CP)	63 393.43
		CF end	-30 680.00	Vehicle (VCU)	1 887 298.53
				Equipment (ECU)	2 230 426.94
				Carbon fixation (CF)	-30 680.00

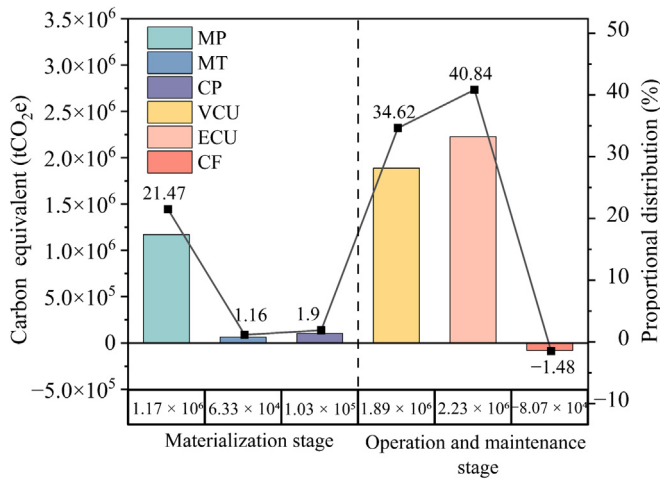


Fig. 4. Distribution of carbon equivalent emissions from the construction materialization stage and operation and maintenance throughout the entire lifecycle.

maintenance stage, infrastructure auxiliary equipment is the primary source, with emissions of 2 230 426.94 tCO₂e, comprising 40.84% of the total lifecycle emissions. Vehicle operation energy consumption contributes 1 887 298.53 tCO₂e, representing 34.62% of the total lifecycle emissions. Overall, the operation and maintenance stage contributes 75.46% of the entire lifecycle emissions, similar to the emission pattern observed in aboveground buildings.

5 Discussion

Based on the carbon emission results in Section 4.3, the carbon emission patterns of each stage of the urban underground highway tunnel facilities were analyzed. Furthermore, energy-saving and emission-reduction measures and suggestions were proposed.

5.1 Carbon emission laws

Figure 5 depicts the temporal trend of carbon emissions from the underground highway tunnel facility. The curve begins with carbon emissions during the construction stage. “CM+VCU” represents the growth trend considering construction and vehicle operation and maintenance stages. “CM+VCU+ECU” includes the growth trend of carbon emissions during construction, vehicle operation and maintenance, and auxiliary facility operation and maintenance stages. “CM+VCU+ECU+CF” indicates the addition of carbon emissions growth during the carbon fixation stage. The demarcation points mark the boundary between the construction period and the operation and maintenance period. The horizontal axis in Fig. 5 reveals a 5-year construction duration and a 100-year operation and maintenance duration. Considering vehicle operation and maintenance, the curve shows a gradual and slow growth in carbon emissions. Incorporating vehicle maintenance and auxiliary equipment maintenance results in a steep curve, indicating a rapid increase in carbon emissions

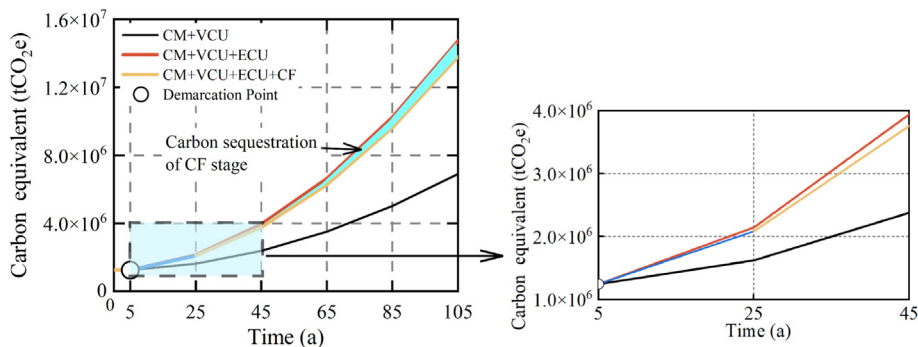


Fig. 5. Carbon emission equivalent of the entire lifecycle of underground highway tunnel facility.

during this stage. During operation and maintenance, carbon emissions from auxiliary equipment are more pronounced. When accounting for carbon fixation during the sub-stage, the shaded area widens over time, indicating the growing importance of plant carbon fixation. The sequestration benefits of the carbon fixation stage contribute to lower final carbon emissions compared to actual emissions, underscoring the crucial role of plant carbon fixation. This aligns with the goal of improving the green and low-carbon development mechanism proposed by the National Development and Reform Commission of China in September 2024.

The carbon emission proportion of each sub-stage of underground highway tunnel facility is shown in Fig. 6. Notably, during the material production sub-stage, steel reinforcement and concrete made significant contributions. The carbon emissions from steel and concrete make up 60.91% and 30.62% of the total carbon emissions from material production activities, respectively. Similarly, the carbon emissions generated by transporting steel bars and concrete account for the majority in the material transportation sub-stage. The two materials together account for 88.25%. This leading carbon emission is attributed to the substantial weight and volume of steel, resulting in increased energy consumption during vehicle transportation. Due to the complexity and self-weight of the shield tunneling machine, the carbon emissions generated during tunnel excavation accounted for 41.35% of the total carbon emissions in the construction process sub-stage. Additionally, the carbon emission equivalent of electricity used in temporary construction facilities closely matches that of tunnel excavation, making up 40.99% of the total carbon emissions from construction process. The data indicate that the key distinction in carbon footprint between underground engineering and aboveground engineering during the construction materialization stage lies in the variance in emissions from excavation engineering. Therefore, particular attention should be given to the carbon emissions stemming from excavation activities in underground engineering.

Figure 6 also presents the proportion of carbon emission equivalents for different types of vehicles during the vehicle carbon consumption sub-stage. Gasoline vehicles exhibit the highest carbon emissions, constituting 78.30% of the overall carbon emissions during vehicle carbon consumption, followed closely by motorcycles, accounting for 9.81% of the total carbon emissions during vehicle carbon consumption. Within the equipment carbon use sub-stage, carbon emissions primarily result from ventilation equipment and lighting equipment within the tunnel. In the equipment carbon use stage, carbon emissions are mainly from the ventilation equipment and lighting equipment in the tunnel, the main reason is that the vehicle and the subway will emit many soot particles and harmful gases in the process of passing through the underground passage, which has an impact on traffic safety, so the ventilation equipment and lighting equipment need to run continuously. Among them, the carbon emissions of tunnel ventilation equipment accounted for the highest proportion, accounting for 89.3% of the total carbon emissions of equipment carbon consumption, and lighting equipment accounted for 10.5% of the total carbon emissions of equipment carbon consumption. Integrating direct air capture technology into ventilation equipment proves crucial in reducing carbon emissions during the operation and maintenance stage and should be considered during the planning and design stages of urban underground highway tunnel facilities.

5.2 Comparison with existing models

Figure 7 compares the boundary delineation of this study with existing research. Studies on calculating the carbon emissions of urban underground highway tunnel facilities using LCA methods remain limited. Therefore, this section contrasts the lifecycle models developed in this study with those by Wang et al. (2025). Both studies conduct a detailed lifecycle boundary division for underground highway tunnel facility and consider energy types and carbon fixation. However, differences arise in boundary scales.

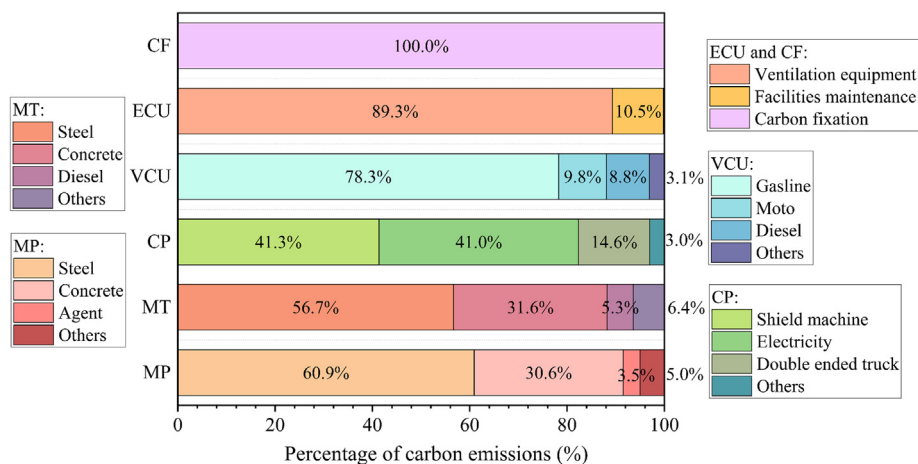


Fig. 6. Proportion of carbon emissions in various stages.

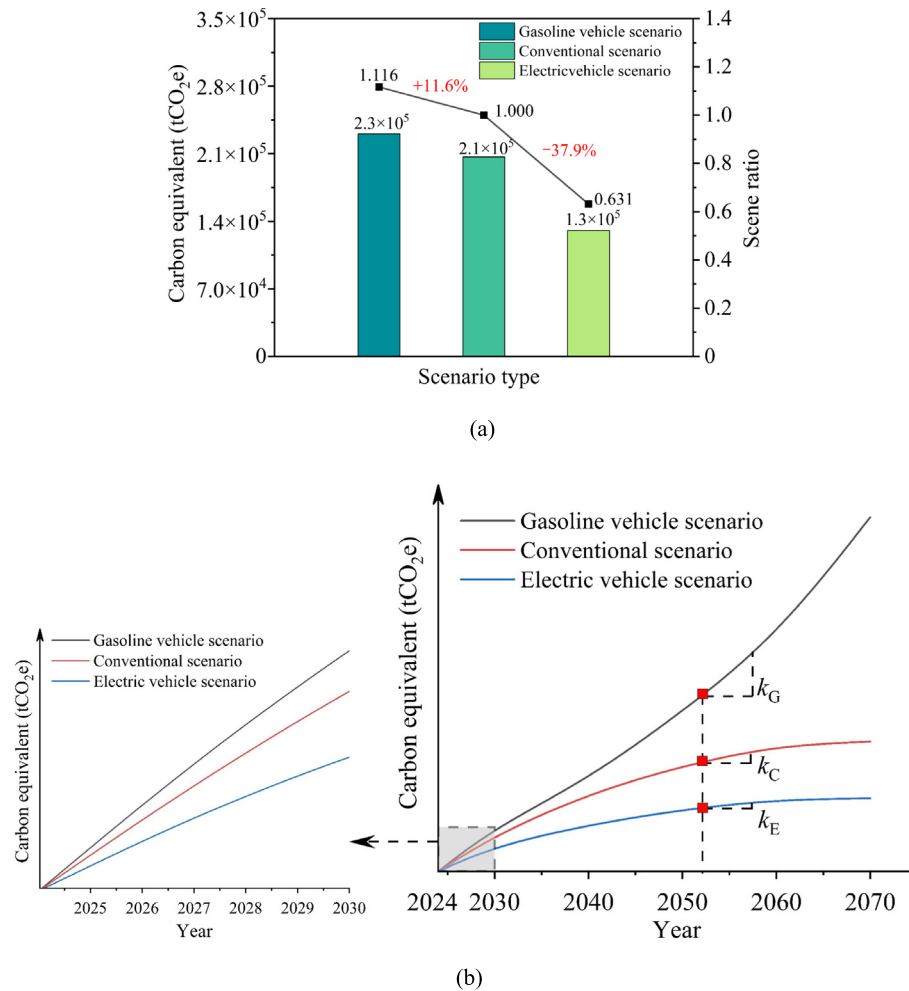


Fig. 8. Comparison of carbon emissions equivalent of vehicle carbon use in three scenarios. (a) Comparison of vehicle carbon emission equivalents in three scenarios, and (b) prediction of vehicle carbon emissions equivalent under three scenarios.

actual scenario. In contrast, when all vehicles are powered by electricity, their carbon emissions are only 0.63 times those of the actual scenario. On the other hand, Fig. 8(b) shows the trend of vehicle carbon emissions under the three scenarios in the future. It can be observed that, whether in the first five years or in the following decades, carbon emissions from gasoline-powered vehicles are the highest, while those from battery-electric vehicles are the lowest. The carbon emission growth rate of gasoline-powered vehicles (k_G) is significantly higher than that of conventional-powered vehicles (k_C) and electric-powered vehicles (k_E).

Based on the above discussion and the existing research, several recommendations are proposed to reduce equipment carbon use and vehicle carbon use emissions. For equipment carbon use, it is suggested to optimize the combination of natural wind and mechanical ventilation. Furthermore, incorporating direct air capture technology into tunnel ventilation systems can help capture carbon emissions from auxiliary equipment (Wang & Wang, 2022). For vehicle carbon use, promoting the use of electric vehicles in urban mobility can yield significant energy savings

(Farzaneh & Jung, 2023). Additionally, developing more underground highway tunnel facilities to release surface space for urban green areas can enhance carbon fixation. Selecting plant species with high carbon absorption capacity and diverse compositions can further improve carbon storage in urban green spaces (Fan et al., 2022; Wang et al., 2021; Wang & Xu, 2023).

The findings of this study offer significant insights for urban policymakers, aiming to reduce the carbon footprint of underground highway tunnel facility. The comprehensive carbon emission calculation model provides a robust tool for guiding policy decisions in the planning, construction, and operation stages. By highlighting the substantial carbon reduction potential of adopting green building materials and transitioning to electric vehicles, this research supports the formulation of targeted emission reduction policies. Furthermore, the integration of carbon fixation technologies and enhanced urban greening initiatives can inform strategies for sustainable urban development, aligning with national carbon neutrality goals. Policymakers can leverage these insights to prioritize investments in

low-carbon technologies and promote regulations that incentivize greener construction practices and energy-efficient highway tunnel facilities.

6 Conclusions

This study presents a carbon emission calculation model for urban underground highway tunnel facilities, developed within the life cycle assessment (LCA) framework. A three-level boundary for carbon footprint calculation is proposed, reflecting the unique characteristics of underground transportation and clearly delineating carbon emission activities during both construction and operation. The model establishes appropriate spatial and temporal scales for carbon footprint assessment. Meanwhile, a detailed database is established for emission factors of various carbon emission activities. The established methodology is applied to a case study in Beijing, revealing both aggregate and individual-stage carbon emission patterns for the urban underground highway tunnel facilities.

The total lifecycle carbon emissions for the studied underground transportation system amount to 5 334 586.45 tCO₂e. The construction materialization stage contributes 23.39% (1 247 540.98 tCO₂e) of the lifecycle emissions, whereas the operation and maintenance stage accounts for 76.61% (4 087 045.47 tCO₂e), establishing it as the predominant emissions stage. Within the construction materialization stage, the material production sub-stage is responsible for the highest emissions, constituting 93.81% of the construction materialization stage and 20.48% of total lifecycle emissions. This underscores the critical need for green, low-carbon building materials. In the operation and maintenance stage, vehicle operation contributes 45.83% of emissions, while auxiliary infrastructure equipment accounts for 54.17%. The integration of carbon fixation technologies alongside natural and mechanical ventilation offers a significant opportunity for emissions reduction. Scenario analyses reveal that a scenario with only gasoline-powered vehicles emits 1.12 times more carbon than the actual scenario, whereas a scenario with only battery-electric vehicles results in emissions at

only 63.15% of the actual level. Thus, the transition from gasoline-powered vehicles to electric vehicles emerges as a vital strategy for energy conservation and emission reduction.

The carbon emission calculation method established in this paper serves as a comprehensive approach for evaluating the lifecycle carbon footprint of urban underground highway tunnel facilities. Its application can contribute significantly to energy conservation and emission reduction at the urban scale.

Data availability

The data that support the findings of this study are available from the corresponding author upon reasonable request.

CRedit authorship contribution statement

Guosheng Wang: Methodology, Conceptualization, Writing – review & editing. **Dechun Lu:** Funding acquisition, Writing – review & editing, Conceptualization. **Gangao Ji:** Writing – original draft, Methodology, Conceptualization. **Xuhua Liang:** Writing – review & editing. **Qingtao Lin:** Funding acquisition, Validation. **Jirui Lv:** Data curation. **Xiuli Du:** Resources, Project administration, Supervision.

Declaration of competing interest

The authors declare that they have no known competing financial interests or personal relationships that could have appeared to influence the work reported in this paper.

Acknowledgement

Support for this study is provided by the National Natural Science Foundation of China (Grant Nos. 52025084, 52378471, and 52208396), and the National Key R&D Program of China (Grant No. 2022YFC3800901).

Appendix A Carbon emission factors**Table A1**

Carbon emission factors of common building materials.

Category of materials		Carbon emission factor
Cement		668 kgCO ₂ e/t
Lime		2190 kgCO ₂ e/t
Glass		1110 kgCO ₂ e/t
Ceramics		14.28 kgCO ₂ e/m ³
Timber		119 kgCO ₂ e/t
Masonry mortar	Composite mortar M2.5	224 kgCO ₂ e/m ³
	Composite mortar M5	236 kgCO ₂ e/m ³
	Composite mortar M7.5	239 kgCO ₂ e/m ³
	Composite mortar M10	234 kgCO ₂ e/m ³
	Cement mortar M2.5	155 kgCO ₂ e/m ³
	Cement mortar M5	165 kgCO ₂ e/m ³
	Cement mortar M7.5	181 kgCO ₂ e/m ³
	Cement mortar M10	200 kgCO ₂ e/m ³
	Cement mortar M15	232 kgCO ₂ e/m ³
Plastering mortar	Cement mortar 1:2	405 kgCO ₂ e/m ³
	Cement mortar 1:3	277 kgCO ₂ e/m ³
	Composite mortar 1:3	285 kgCO ₂ e/m ³
	Lime mortar 1:2.5	342 kgCO ₂ e/m ³
	Lime mortar 1:3	293 kgCO ₂ e/m ³
Concrete	C30	297 kgCO ₂ e/m ³
	C40	326 kgCO ₂ e/m ³
	C50	353 kgCO ₂ e/m ³
	C60	411 kgCO ₂ e/m ³
Steel	Large steel	270 kgCO ₂ e/t
	Small and medium-sized steels	2137 kgCO ₂ e/t
	Wire rod	2140 kgCO ₂ e/t
	Hot rolled strip	2246 kgCO ₂ e/t
	Stainless steel	6130 kgCO ₂ e/t
Aluminum	Aluminum ingots	11.142 tCO ₂ e/t
	Strip	11.782 tCO ₂ e/t
	Aluminum foil	12.492 tCO ₂ e/t
	Aluminum extrusions	11.87 tCO ₂ e/t

Table A2
Carbon emission factors for different modes of transport.

Category of shipping method	Carbon emission factor (kgCO ₂ e/(t·km))	Category of shipping method	Carbon emission factor (kgCO ₂ e/(t·km))
Light diesel truck transportation (2t)	0.286	Light gasoline truck transportation (2 t)	0.334
Medium-sized diesel truck transportation (8t)	0.179	Medium-sized gasoline Truck transportation (8 t)	0.115
Heavy diesel truck transportation (10t)	0.162	Heavy gasoline truck transportation (10 t)	0.104
Heavy diesel truck transportation (18t)	0.129	Heavy gasoline truck transportation (18 t)	0.104
Heavy diesel truck transportation (30t)	0.078	Electric locomotive transportation	0.010
Heavy diesel truck transportation (46t)	0.057	Diesel locomotives transportation	0.011

Table A3
Carbon emission factors of common machinery and equipment.

Machine name	Specifications and models	Carbon emission factor
Track-type bulldozer	Power: 75 kw	21.94 kgCO ₂ e/h
	Power: 105 kw	23.61 kgCO ₂ e/h
	Power: 135 kw	25.94 kgCO ₂ e/h
Crawler single-bucket hydraulic excavator	Bucket capacity: 0.6 m ³	13.08 kgCO ₂ e/h
	Bucket capacity: 1.0 m ³	24.46 kgCO ₂ e/h
Anchor bolt drilling machine	Bolt diameter: 32 mm	27.07 kgCO ₂ e/h
Crawler diesel pile driver	Impact quality: 2.5 t	17.23 kgCO ₂ e/h
	Impact quality: 3.5 t	18.62 kgCO ₂ e/h
	Impact quality: 5 t	20.94 kgCO ₂ e/h
Electric tamping machine	Consolidate energy: 250 N·m	2.20 kgCO ₂ e/h
Self-elevating tower crane	Improve quality: 400 t	21.73 kgCO ₂ e/h
	Improve quality: 800 t	22.37 kgCO ₂ e/h
	Improve quality: 1000 t	22.49 kgCO ₂ e/h
Forklift cranes	Improve quality: 3.0 t	9.65 kgCO ₂ e/h
Trucks	Load: 4.0 t	9.29 kgCO ₂ e/h
Tanker	EQ5167GPSBDC9	11.51 kgCO ₂ e/h
Shield machine	–	3569.05 kgCO ₂ e/m
Temporary facilities	–	1.058 kgCO ₂ e/kWh

Table A4
Carbon emission factors for fuel energy.

Fuel classification	Carbon emission factor	Fuel classification	Carbon emission factor
Raw coal	1.834 kgCO ₂ e/kg	Fuel oil	3.167 kgCO ₂ e/kg
Washed coal	2.311 kgCO ₂ e/kg	Naphtha	3.198 kgCO ₂ e/kg
Coal gangue	0.730 kgCO ₂ e/kg	Lube	2.986 kgCO ₂ e/kg
Coke	2.733 kgCO ₂ e/kg	Paraffin	2.893 kgCO ₂ e/kg
Coke oven gas	0.625 kgCO ₂ e/m ³	Solvent oils	3.111 kgCO ₂ e/kg
Blast furnace gas	0.824 kgCO ₂ e/m ³	Petroleum asphalt	2.707 kgCO ₂ e/kg
Converter gas	1.152 kgCO ₂ e/m ³	Petroleum coke	2.656 kgCO ₂ e/kg
Other gas	0.195 kgCO ₂ e/m ³	Liquefied petroleum gas	3.094 kgCO ₂ e/kg
Crude	2.983 kgCO ₂ e/kg	Refinery dry gas	2.222 kgCO ₂ e/m ³
Gasoline	2.917 kgCO ₂ e/kg	Other petroleum	3.029 kgCO ₂ e/kg
Kerosene	3.107 kgCO ₂ e/kg	Natural gas	2.115 kgCO ₂ e/m ³
Diesel fuel	3.107 kgCO ₂ e/kg	Liquefied natural gas	2.802 kgCO ₂ e/kg

Table A5
Carbon emission factors for different types of fuel.

Vehicle Category	Gasoline	Diesel	Hybrid	Natural gas	Electric	Motorcycle
Carbon emission factor (kgCO ₂ e/(h·km))	0.2645	0.3691	0.2208	0.1115	0.1496	0.1196

Table A6
Total energy consumption and carbon emission factors of lighting equipment per unit length.

Design speed (km/h)	Total energy consumption (kW/(h·km))	Carbon emission factors (kgCO ₂ e/(h·km))	
		Two-lane	Four lanes and above
40	12.45	7.28	14.56
60	18.75	10.96	21.93
80	24.90	14.56	29.13

Table A7
Total energy consumption and carbon emission factors of ventilation equipment per unit length.

Number of groups arranged	Total energy consumption (kW/(h·km))	Carbon emission factors (kgCO ₂ e/(h·km))
1	330	193.05
2	660	386.10
3	990	579.15

Table A8
Carbon fixation factors (CSF) of different types of vegetation.

Vegetation types	Attached green space	Park green space	Protective green space	Regional green space
CSF (kgCO ₂ e/(m ² ·a))	0.5578	0.6136	0.4686	0.8343

References

- Aye, L., Ngo, T., Crawford, R. H., Gammampila, R., & Mendis, P. (2012). Life cycle greenhouse gas emissions and energy analysis of prefabricated reusable building modules. *Energy and Buildings*, 47, 159–168.
- Barles, S. (2009). Urban metabolism of Paris and its region. *Journal of Industrial Ecology*, 13(6), 898–913.
- Beijing Transport Institute. (2021). *2021 annual report on Beijing transportation development* [Research report]. Beijing: Beijing Transport Institute. (in Chinese).
- Center for Strategic Studies of the Chinese Academy of Engineering, Underground Space Branch of the China Institute of Rock Mechanics and Engineering, & Chinese Society of Urban Planning (2022). *2022 blue book of urban underground space*. Beijing: Science Press (in Chinese).
- Chen, G. Q., Chen, H., Chen, Z. M., Zhang, B., Shao, L., Guo, S., Zhou, S. Y., & Jiang, M. M. (2011). Low-carbon building assessment and multi-scale input-output analysis. *Communications in Nonlinear Science and Numerical Simulation*, 16(1), 583–595.
- Chen, J., Liu, X. J., & Yao, G. Z. (2017). Evaluation of the implementation effect of the tidal flow lane on Chaoyang road in Beijing. In *Proceedings of the 12th China annual conference on intelligent transportation systems* (pp. 170–179) (in Chinese).
- Chen, P., Zhang, L., Wang, Y., Fang, Y., Zhang, F., & Xu, Y. (2021). Environmentally friendly utilization of coal gangue as aggregates for shotcrete used in the construction of Coal Mine Tunnel. *Case Studies in Construction Materials*, 15.
- China Automotive Data Co., Ltd. (2020). *Research report on China's low-carbon action plan for the automotive industry 2020*. Tianjin: China Automotive Data Co., Ltd. 16–17. (in Chinese).
- China Merchants Chongqing Transportation Research and Design Institute. (2014). *JTG/T D70/2-01—2014. Detailed rules for the lighting design of highway tunnels* (in Chinese).
- Cole, R. J. (1998). Energy and greenhouse gas emissions associated with the construction of alternative structural systems. *Building and Environment*, 34(3), 335–348.
- Fan, W., Huang, S., Yu, Y., Xu, Y., & Cheng, S. (2022). Decomposition and decoupling analysis of carbon footprint pressure in China's cities. *Journal of Cleaner Production*, 372, 133792.
- Farzaneh, F., & Jung, S. (2023). Lifecycle carbon footprint comparison between internal combustion engine versus electric transit vehicle: A case study in the U.S. *Journal of Cleaner Production*, 390, 136111.
- Fenner, A. E., Kibert, C. J., Woo, J., Morque, S., Razkenari, M., & Hakim, H. (2018). The carbon footprint of buildings: A review of methodologies and applications. *Renewable and Sustainable Energy Reviews*, 94, 1142–1152.
- Finkbeiner, M., Inaba, A., Tan, R., Christiansen, K., & Klüppel, H.-J. (2006). The new international standards for life cycle assessment: ISO 14040 and ISO 14044. *The International Journal of Life Cycle Assessment*, 11(2), 80–85.
- Gao, C., Niu, J., & Xing, X. (2021). *Methods for measuring building carbon emissions and calculating emission factors*. Jilin University Press (in Chinese).
- Ghafoori, M., & Abdallah, M. (2022). Innovative Optimization Model for planning upgrade and maintenance interventions for buildings. *Journal of Performance of Constructed Facilities*, 36(6).
- Ghate, A. T., & Qamar, S. (2020). Carbon footprint of urban public transport systems in Indian cities. *Case Studies on Transport Policy*, 8(1), 245–251.
- Guo, J., Zhang, W., Zhang, J., Xie, L., Zeng, X., & Zhong, J. (2024). Carbon reduction measures-based life cycle assessment of the photo-voltaic-supported sewage treatment system. *Sustainable Cities and Society*, 101, 105074.
- Gustavsson, L., Joelsson, A., & Sathre, R. (2010). Life cycle primary energy use and carbon emission of an eight-storey wood-framed apartment building. *Energy and Buildings*, 42(2), 230–242.
- Joensuu, T., Leino, R., Heinonen, J., & Saari, A. (2022). Developing buildings' life cycle assessment in circular economy-comparing methods for assessing carbon footprint of reusable components. *Sustainable Cities and Society*, 77, 103499.
- Lee, J.-Y., Lee, C.-K., & Chun, Y.-Y. (2020). Greenhouse gas emissions from high-speed rail infrastructure construction in Korea. *Transportation Research Part D: Transport and Environment*, 87, 102514.
- Li, C., Li, K., & Chen, Z. (2008). Service life prediction of underground structures: A case study on the transport hub of Tianjin station. *Advances in Concrete Structural Durability: Proceedings of ICDCS, 2008*(1), 985–991.
- Li, S., Huang, M., Cui, M., Xu, K., & Jin, G. (2023). Thermal and mechanical properties of bio-cemented quartz sand mixed with steel slag. *Biogeotechnics*, 1(3), 100036.
- Li, X., Tan, X., Wu, R., Xu, H., Zhong, Z., & Li, Y. (2021). Paths for carbon peak and carbon neutrality in transport sector in China. *Chinese Journal of Engineering Science*, 23(6), 15.
- Li, Y., He, Q., Luo, X., Zhang, Y., & Dong, L. (2018). Calculation of life-cycle greenhouse gas emissions of urban rail transit systems: A case study of shanghai metro. *Resources, Conservation and Recycling*, 128, 451–457.
- Li, Y. Y., & Chen, J. (2020). *The carbon footprint of the building throughout its lifecycle*. China Architecture & Building Press (in Chinese).
- Liu, J., Han, K., Chen, X. (Michael), & Ong, G. P. (2019). Spatial-temporal inference of urban traffic emissions based on taxi trajectories and multi-source Urban Data. *Transportation Research Part C: Emerging Technologies*, 106, 145–165.
- Liu, Y. (2023). Study on the ventilation scheme and control measures for extra-long tunnels. *Automation Application*, 64(16), 1–3 (in Chinese).
- Ministry of Housing and Urban-Rural Development of the People's Republic of China, & State Administration for Market Regulation. (2019). *GBT 51366—2019: Standard for building carbon emission calculation*. (in Chinese).
- Mohamed, M. A. A. (2019). Saving energy through using Green Rating System for building commissioning. *Energy Procedia*, 162, 369–378.
- Nyhan, M., Sobolevsky, S., Kang, C., Robinson, P., Corti, A., & Szell, M. (2016). Predicting vehicular emissions in high spatial resolution using pervasively measured transportation data and microscopic emissions model. *Atmospheric Environment*, 140, 352–363.
- Pan, D., Yu, X., & Zhou, Y. (2023). Cradle-to-grave lifecycle carbon footprint analysis and frontier decarbonization pathways of district buildings in subtropical Guangzhou, China. *Journal of Cleaner Production*, 416, 137921.
- Peng, F.-L., Qiao, Y.-K., Sabri, S., Atazadeh, B., & Rajabifard, A. (2021). A collaborative approach for urban underground space development toward sustainable development goals: Critical dimensions and future directions. *Frontiers of Structural and Civil Engineering*, 15(1), 20–45.
- Peng, Y., Wang, Y., Chen, H., Wang, L., Luo, B., & Tong, H. (2024). Carbon reduction potential of a rain garden: A cradle-to-grave life cycle carbon footprint assessment. *Journal of Cleaner Production*, 434, 139806.
- Pérez, J., Lumbreras, J., Rodríguez, E., & Vedrenne, M. (2017). A methodology for estimating the carbon footprint of waste collection vehicles under different scenarios: Application to Madrid. *Transportation Research Part D: Transport and Environment*, 52, 156–171.
- Prather, M. J., Penner, J. E., Fuglestvedt, J. S., Kurosawa, A., Lowe, J. A., & Höhne, N. (2009). Tracking uncertainties in the causal chain from human activities to climate. *Geophysical Research Letters*, 36(5).
- Pi, Y. H. (2016). *Study on calculating carbon emissions of shield tunnel construction* [Doctoral dissertation, Nanchang University]. (in Chinese).
- Qi, Y., Rao, G., Zha, L., Chen, L., & Niu, Y. (2022). Carbon transfer decision model based on LMDI method. *Computational Intelligence and Neuroscience*, 2022, 1–9.
- Qiao, Y., Le, P. F., Dong, Y., & Lu, C. F. (2024). Planning an adaptive reuse development of underutilized urban underground infrastructures: A case study of Qingdao, China. *Underground Space*, 14, 18–33.
- Qiao, Y.-K., Peng, F.-L., Sabri, S., & Rajabifard, A. (2019). Low carbon effects of urban underground space. *Sustainable Cities and Society*, 45, 451–459.
- Ramírez, A. L., & Korkkiala-Tanttu, L. (2023). Stabilisation of Malmi soft clay with traditional and low-CO₂ binders. *Transportation Geotechnics*, 38, 100920.
- Richard, K., & Li, H. Z. (2001). *Pareto 80/20 rule*. Beijing: Haichao Press (in Chinese).
- Shau, H.-J., Liu, T.-Y., Chen, P.-H., & Chou, N. N. (2019). Sustainability practices for the Suhua highway improvement project in Taiwan. *International Journal of Civil Engineering*, 17(10), 1631–1641.
- Sim, J., & Sim, J. (2017). The atmospheric environmental impact of a Korean traditional building's life cycle, along with carbon footprint analysis. *Sustainable Cities and Society*, 28, 172–186.

- Su, X., Huang, Y., Chen, C., Xu, Z., Tian, S., & Peng, L. (2023). A dynamic life cycle assessment model for long-term carbon emissions prediction of buildings: A passive building as case study. *Sustainable Cities and Society*, *96*, 104636.
- Teng, J., & Wu, X. (2014). Eco-footprint-based life-cycle eco-efficiency assessment of building projects. *Ecological Indicators*, *39*, 160–168.
- Traffic Management Bureau of the Ministry of Public Security. (2023). *The total number of motor vehicles in China reached 417 million, with over 500 million drivers and 13.1 million new energy vehicles, a year-on-year increase of 67.13%*. (in Chinese).
- Verma, M., Dev, N., Rahman, I., Nigam, M., Ahmed, M., & Mallick, J. (2022). Geopolymer concrete: A material for sustainable development in Indian construction industries. *Crystals*, *12*(4), 514.
- Wang, G., Li, Z., Liang, J., Lu, D., & Du, X. (2024). A state-dependent non-orthogonal elastoplastic constitutive model for sand. *Computers and Geotechnics*, *166*, 105960.
- Wang, J., Duan, H., Chen, K., Chan, I. Y. S., Xue, F., & Zhang, N. (2025). Role of urban underground-space development in achieving carbon neutrality: A national-level analysis in China. *Engineering*, *45*, 212–221.
- Wang, X., & Wang, H. L. (2022). *Introduction to carbon neutral technologies*. Beijing: Higher Education Press (in Chinese).
- Wang, Y., Chang, Q., & Li, X. (2021). Promoting sustainable carbon sequestration of plants in urban greenspace by planting design: A case study in parks of Beijing. *Urban Forestry & Urban Greening*, *64*, 127291.
- Wang, Y. G., Xu, G. Q., Bai, M., et al. (2023). Comparison of structural characteristics and carbon sink functions between trees, shrubs and herbs of coniferous and broadleaf forests in Wushan. *Journal of Central South University of Forestry & Technology*, *43*(10), 98–106 (in Chinese).
- Wu, H., Zhou, W., Bao, Z., Long, W., Chen, K., & Liu, K. (2024). Life cycle assessment of carbon emissions for cross-sea tunnel: A case study of Shenzhen-Zhongshan bridge and tunnel in China. *Case Studies in Construction Materials*, *21*.
- Xu, F., Wang, X., & Li, L. (2023). NPP and vegetation carbon sink capacity estimation of urban green space using the optimized CASA model: A case study of five Chinese cities. *Atmosphere*, *14*(7), 1161.
- Zhang, Y. S. (2002). *Assessment of carbon dioxide reduction during the life cycle of buildings* [Doctoral dissertation]. National Cheng Kung University. (in Chinese).
- Zhao, L., Hu, S., Wang, D., Guo, Y., & Fu, C. (2022). Evaluation of the effects of tunnel lighting environment on energy consumption and drivers' reaction time. *Advances in Materials Science and Engineering*, *2022*, 1–13.
- Zou, L. (2013). *Research on the reliability of LED lamps affecting factors and evaluation method* [Doctoral dissertation, Dalian Polytechnic University]. Dalian Polytechnic University. (in Chinese)